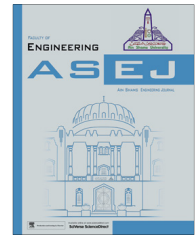




Ain Shams University  
Ain Shams Engineering Journal

www.elsevier.com/locate/asej  
www.sciencedirect.com



## MECHANICAL ENGINEERING

# Entropy generation due to micropolar fluid flow between concentric cylinders with slip and convective boundary conditions

D. Srinivasacharya \*, K. Hima Bindu

Department of Mathematics, National Institute of Technology, Warangal 506004, India

Received 23 May 2015; revised 15 September 2015; accepted 27 October 2015

## KEYWORDS

Concentric cylinders;  
Micropolar fluid;  
Spectral quasilinearization;  
Entropy;  
Bejan number

**Abstract** In this study, the entropy generation of micropolar fluid flow through concentric cylindrical annulus associated with slip and convective boundary conditions is performed numerically. The fluid flow in an annulus is due to the rotation of the outer cylinder with constant velocity. The analysis of such kind of fluid flow is governed by nonlinear partial differential equations. In the present study these equations are solved using the spectral quasilinearization method. The resultant velocity, microrotation and temperature distributions from the spectral quasi linearization method are used to evaluate the entropy generation rate and the Bejan number. Further the impact of boundary conditions on the entropy generation is also presented.

© 2015 Faculty of Engineering, Ain Shams University. Production and hosting by Elsevier B.V. This is an open access article under the CC BY-NC-ND license (<http://creativecommons.org/licenses/by-nc-nd/4.0/>).

## 1. Introduction

Fluid flow and heat transfer inside a cylindrical annular space through convection have many significant engineering applications. This type of fluid flow is observed in rotating electrical machines, swirl nozzles, rotating disks, standard commercial rheometers, and other chemical and mechanical mixing equipments. In practical situations, many factors affect the flow and

heat transfer through annular space. Considerable research studies were carried out to investigate the Newtonian and non-Newtonian fluid flow through concentric cylinders. Taylor [1] studied theoretically and experimentally the flow of viscous incompressible fluid between two concentric cylinders. Hesami et al. [2] analyzed laminar mixed convection flow pattern and heat transfer for air inside a vertical cylindrical annular space. Borjini et al. [3] studied the effect of radiation on unsteady numerical convection between two horizontal concentric and vertically eccentric cylinders. Atayilmaz [4] carried out both numerical and experimental analysis on natural convection of heat transfer from horizontal concentric cylinders. Deka and Paul [5] studied the viscous flow between two porous concentric circular cylinders with radial flow and a constant heat flux at the inner cylinder.

Most of the industrial and engineering flow processes and thermal systems are unable to perform optimally due to entropy generation. It is important to establish the factors that

\* Corresponding author. Tel.: +91 870 2462821; fax: +91 870 2459547.

E-mail addresses: [dsrinivasacharya@yahoo.com](mailto:dsrinivasacharya@yahoo.com), [dsc@nitw.ac.in](mailto:dsc@nitw.ac.in) (D. Srinivasacharya).

Peer review under responsibility of Ain Shams University.



Production and hosting by Elsevier

<http://dx.doi.org/10.1016/j.asej.2015.10.016>

2090-4479 © 2015 Faculty of Engineering, Ain Shams University. Production and hosting by Elsevier B.V.

This is an open access article under the CC BY-NC-ND license (<http://creativecommons.org/licenses/by-nc-nd/4.0/>).

Please cite this article in press as: Srinivasacharya D, Hima Bindu K, Entropy generation due to micropolar fluid flow between concentric cylinders with slip and convective boundary conditions, Ain Shams Eng J (2016), <http://dx.doi.org/10.1016/j.asej.2015.10.016>

**Nomenclature**

$a$	radius of the inner cylinder	$Re$	Reynolds number
$b$	radius of the outer cylinder	$T_p$	dimensionless temperature difference
$Be$	Bejan number	<i>Greek symbols</i>	
$Bi$	Biot number	$\alpha$	slip parameter
$Br$	Brinkman number	$\beta, \gamma$	gyration viscosity coefficients
$g^*$	acceleration due to gravity	$\kappa$	vortex viscosity
$g_s$	buoyancy parameter	$\rho$	density of the fluid
$Gr$	Grashof number	$\Gamma$	dimensionless microrotational component
$K_f$	thermal conductivity	$\theta$	dimensionless temperature
$m^2$	micropolar parameter	$\mu$	viscosity of the fluid
$N$	coupling number	<i>Superscript</i>	
$N_v$	entropy generation due to viscous dissipation	$'$	differentiation with respect to $\lambda$
$N_h$	entropy generation due to heat transfer		
$N_s$	dimensionless entropy generation		

contribute to entropy generation. The established factors are to be minimized, thus optimizing the energy resources and flow system efficiency. Entropy analysis is a technique to quantify the thermodynamic irreversibility in any fluid flow and heat transfer processes, which is an outcome of second law of thermodynamics. Entropy generation is a measure of the amount of irreversibility associated with the real processes. Different factors that affect the entropy generation are heat transfer across finite temperature gradient, characteristic of convective heat transfer, viscous effects, etc. Entropy generation destroys the available energy of a system and as a result, imposes considerable extra costs to any thermal system.

The concept of entropy generation minimization is developed by Bejan [6]. Several researchers investigated the entropy generation on fluid flows through concentric cylinders. Sahin [7] investigated the entropy generation for a viscous fluid flow in a duct subjected to constant surface temperature. Tasnim and Mahmud [8] studied the entropy generation in a vertical concentric channel with isothermal boundary conditions. Haddad et al. [9] presented the entropy generation due to laminar forced convection in the entrance region of a concentric cylindrical annulus. It was found that the thermal entropy generation is relatively dominant over viscous entropy generation. Yari [10] studied the second-law analysis and entropy generation for heat transfer and fluid flow through microannulus by considering the viscous dissipation effect, slip velocity and temperature jump. Chen et al. [11] analyzed the natural convection and entropy generation in a vertically concentric annular space. Assad and Oztop [12] presented the effect of internal heat generation on entropy generation between two rotating cylinders. Mazgar et al. [13] studied the entropy generation through combined non-gray gas radiation and mixed convection within a concentric cylindrical annulus. Egunjobi and Makinde [14] investigated the entropy generation rate in transient Couette flow of variable viscosity fluid between two concentric pipes where inner pipe is moving and outer pipe is fixed. Rashidi et al. [15] studied the effects of magnetic interaction number, slip factor and relative temperature difference on velocity and temperature profiles as well as entropy generation in magnetohydrodynamic (MHD) flow of a fluid with variable properties over a rotating disk. Das et al. [16] analyzed the

entropy generation in a Couette flow caused due to the movement of the upper channel wall with suction/injection in rotating frame of reference.

Few studies on entropy generation are related to non-Newtonian fluids. Yilbas et al. [17] studied the entropy analysis for non-Newtonian fluid flow in annular Pipe. They found that the rate of entropy generation can be reduced by reducing both non-Newtonian parameter and Brinkman number. Kahraman and Yurusoy [18] examined the entropy generation due to non-Newtonian fluid flow in an annular pipe with relative rotation using a third-grade fluid model. Mirzazadeh et al. [19] have focused on the entropy generation induced by the flow of a non-linear viscoelastic fluid between concentric rotating cylinders. Their results showed that the entropy generation number increases with increase in Brinkman number. Mahian et al. [20] studied the entropy generation due to flow and heat transfer of nanofluids between corotating cylinders with constant heat flux on the walls. Kim et al. [21] investigated numerically the entropy generation in a U-shaped Pulsating Heat Pipe. Chen et al. [22] studied numerically the heat transfer and entropy generation within a fully developed mixed convection flow of  $Al_2O_3$ -water nanofluid in a vertical channel. Mkwizu and Makinde [23] investigated Brownian motion, thermophoresis and variable viscosity on entropy generation of nanofluid flow through a parallel channel with convective cooling. Das et al. [24] examined the entropy generation on pseudo-plastic nanofluid flow through a porous channel under the MHD effect with convective heating.

The non-Newtonian fluids, which include colloidal fluids, heterogeneous mixtures, exotic lubricants, animal blood, most slurries, and some liquids with polymer additives have microstructure and therefore do not follow the Newtonian fluid flow theory. In order to explore and understand the behavior of such fluids there were many non-Newtonian fluid theories established. Among these, micropolar fluid theory introduced by Eringen [25] has distinct features, such as microscopic effects arising from the local structure, micro motion of fluid elements, presence of couple stresses, body couples and non-symmetric stress tensor. Thus, it can be used to study the behavior of exotic lubricants, colloidal suspensions or polymeric additives, blood flow, liquid crystals and dirty oils.

Although the analysis of entropy generation in a micropolar fluid is important, very little work has been reported in the literature. Chen et al. [26] considered the problem of entropy generation due to micropolar fluid flow along the wavy surface with radiation effect. Ramana Murthy and Srinivas [27] analyzed the entropy generation on the steady Poiseuille flow of two immiscible incompressible micropolar fluids between two horizontal parallel plates of a channel with constant wall temperatures in terms of entropy generation.

Though, most of the work has been done on entropy generation, to the best knowledge of the authors, entropy generation analysis for micropolar fluid flow with slip and convective boundary condition has not yet been addressed in the literature. The slip over a moving surface is mainly caused by the two effects, i.e., surface roughness and rarefaction of the fluid. This type of flow is commonly encountered in many engineering aspects, such as high altitude flight, micro-machines, vacuum technology and aerosol reactors. The slip dependent velocity implies the reduction in mechanical energy, which is converted into thermal energy, thus reducing the entropy generation. Further, by relating entropy generation to slip factor on the flow and heat field solutions gives more accurate results. This analysis helps the designer for the better efficiency calculations and geometrical optimization of rotating systems.

Thus, the aim of the present paper is to study the entropy generation rate of micropolar fluid flow through concentric cylinders with slip and convective boundary conditions.

## 2. Mathematical formulation

Consider a steady, laminar, incompressible micropolar fluid in an annulus between infinite vertical concentric circular cylinders of radii  $a$  and  $b$  ( $a < b$ ). Choose the cylindrical polar coordinate system  $(r, \varphi, z)$  with  $z$ -axis as the common axis for both cylinders (as shown in Fig. 1). The inner is at rest and outer cylinder is rotating with constant angular velocity  $\Omega$ . The flow is generated due to rotation of the outer cylinder. Since the flow is fully developed and the cylinders are of infinite length, the flow depends only on  $r$ . The temperature of

the fluid is assumed to be  $T_a$ . The slip and convective boundary conditions are applied at the inner and outer cylinders. Further, assume that except density all the fluid properties are constant in the buoyancy term of the balance of momentum equation. With the above assumptions and Boussinesq approximations with energy, the equations governing the steady flow of an incompressible micropolar fluid [28,29] are as follows:

$$\frac{\partial u}{\partial \varphi} = 0 \quad (1)$$

$$\frac{\partial p}{\partial r} = \frac{\rho u^2}{r} \quad (2)$$

$$-\kappa \frac{\partial \Gamma}{\partial r} + (\mu + \kappa) \left( \frac{1}{r} \frac{\partial u}{\partial r} - \frac{u}{r^2} + \frac{\partial^2 u}{\partial r^2} \right) + \rho g^* \beta_T (T - T_a) = 0 \quad (3)$$

$$-2\kappa \Gamma + \kappa \left( \frac{\partial u}{\partial r} + \frac{u}{r} \right) + \gamma \left( \frac{1}{r} \frac{\partial \Gamma}{\partial r} + \frac{\partial^2 \Gamma}{\partial r^2} \right) = 0 \quad (4)$$

$$K_f \left( \frac{1}{r} \frac{\partial T}{\partial r} + \frac{\partial^2 T}{\partial r^2} \right) + 2\kappa \left( \frac{1}{2r} \frac{\partial (ru)}{\partial r} - \Gamma \right)^2 + (\mu + \kappa) \left( \frac{\partial u}{\partial r} - \frac{u}{r} \right)^2 + \gamma \left( \frac{\partial \Gamma}{\partial r} \right)^2 = 0 \quad (5)$$

where  $u$  is velocity in  $\varphi$  direction,  $\Gamma$  is microrotation,  $T$  is the temperature,  $\rho$  is fluid density,  $\mu$  is dynamic coefficient of viscosity,  $\kappa$  is vortex viscosity,  $\gamma$  is the spin gradient viscosity,  $g^*$  is the acceleration due to gravity,  $\beta_T$  is the coefficient of thermal expansion, and  $K_f$  is the thermal conductivity.

The boundary conditions are

$$u = \alpha' \left[ \frac{\partial u}{\partial r} - \frac{u}{r} \right], \quad \Gamma = 0, \quad K_f \frac{\partial T}{\partial r} - h_1 (T - T_a) = 0, \quad \text{at } r = a \quad (6a)$$

$$u = b\Omega - \alpha' \left[ \frac{\partial u}{\partial r} - \frac{u}{r} \right], \quad \Gamma = \frac{1}{2r} \frac{\partial}{\partial r} (ru), \quad K_f \frac{\partial T}{\partial r} + h_2 (T - T_b) = 0, \quad \text{at } r = b \quad (6b)$$

where  $\alpha'$  slip length of the inner and outer cylinders,  $h_1, h_2$  are the convective heat transfer coefficients of the inner and outer cylinders and  $T_b$  is the ambient temperature.

Introducing the following transformations

$$r = b\sqrt{\lambda}, \quad u = \frac{\Omega}{\sqrt{\lambda}} f(\lambda), \quad \Gamma = \frac{\Omega}{b} g(\lambda), \quad T - T_a = (T_b - T_a) \theta(\lambda) \quad (7)$$

in Eqs. (3)–(5), we get

$$-\frac{2N}{1-N} \lambda g' + \frac{4\lambda}{1-N} f'' + \sqrt{\lambda} g_s \theta = 0 \quad (8)$$

$$-g + f' + \frac{2(2-N)}{m^2} (g' + \lambda g'') = 0 \quad (9)$$

$$(\lambda^3 \theta'' + \lambda^2 \theta') + \frac{Br}{1-N} \left[ (N/2) \lambda^2 (f' - g)^2 + (f - \lambda f')^2 + \frac{N(2-N)}{m^2} \lambda^3 g^2 \right] = 0 \quad (10)$$

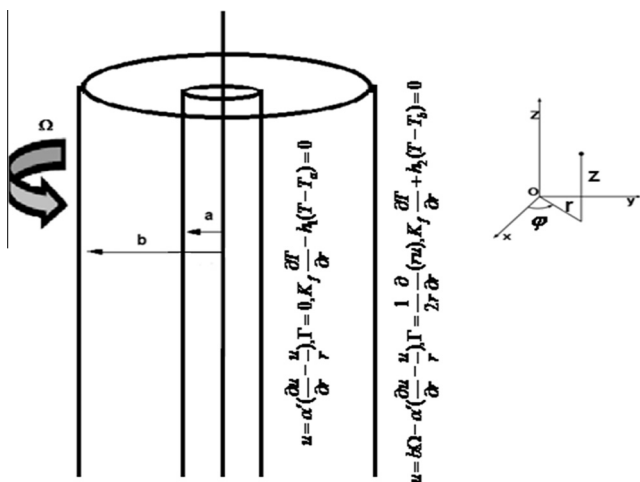


Figure 1 Schematic diagram of the problem.

where primes denote differentiation with respect to the variable  $\lambda$ ,  $N = \frac{\kappa}{\mu + \kappa}$  is coupling number,  $Re = \frac{\rho \Omega b}{\mu}$  is the Reynolds number,  $Gr = \frac{g^* \beta_T (T_b - T_a) b^3}{\nu^2}$  is the Grashof number,  $Br = \frac{\Omega^2 \mu}{K_f (T_b - T_a)}$  is the Brinkman number, and  $m^2 = \frac{b^2 \kappa (2\mu + \kappa)}{\gamma (\mu + \kappa)}$  is micropolar parameter.  $g_s = \frac{Gr}{Re}$  is the buoyancy parameter.

The corresponding boundary conditions in dimensionless form are as follows:

$$\begin{aligned} -2\alpha\lambda_0 f'(\lambda_0) + (\sqrt{\lambda_0} + 2\alpha)f(\lambda_0) &= 0, \quad g(\lambda_0) = 0, \\ Bi_1 \theta(\lambda_0) &= 2\sqrt{\lambda_0} \theta'(\lambda_0), \quad \text{where } \lambda_0 = \left(\frac{a}{b}\right)^2 \\ 2\alpha f'(1) + (1 - 2\alpha)f(1) &= b, \quad g(1) = \left[\frac{df}{d\lambda}\right]_{\lambda=1}, \\ Bi_2(1 - \theta(1)) &= 2\theta'(1) \end{aligned} \quad (11)$$

where  $\alpha = \frac{\alpha'}{b}$  is the slip coefficient, and  $Bi_i = \frac{bh_i}{K_f}$  is the Biot number for each cylinder. Sub indexes  $i = 1, 2$  refer to the inner and outer cylinders, respectively. In general Biot number assumed to be same for the two cylinders.

### 3. Method of solution

The system of Eqs. (8)–(10) along with the boundary conditions (11) are solved using the quasilinearization method. This quasilinearization method (QLM) is a generalization of the Newton–Raphson method and was proposed by Bellman and Kalaba [30] for solving nonlinear boundary value problems. In this method the iteration scheme is obtained by linearizing the nonlinear component of a differential equation using the Taylor series expansion.

Let the  $f_r$ ,  $g_r$  and  $\theta_r$  be an approximate current solution and  $f_{r+1}$ ,  $g_{r+1}$  and  $\theta_{r+1}$  be an improved solution of the system of Eqs. (8)–(10). By taking Taylor's series expansion of nonlinear terms in (8)–(10) around the current solution and neglecting the second and higher order derivative terms, we get the linearized equations as follows:

$$a_{1,r} f_{r+1}'' - a_{2,r} g_{r+1}' + a_{3,r} \theta_{r+1} = 0 \quad (12)$$

$$f_{r+1}' + b_{1,r} g_{r+1}'' + b_{2,r} g_{r+1}' - g_{r+1} = 0 \quad (13)$$

$$\begin{aligned} c_{1,r} \theta_{r+1}'' + c_{2,r} \theta_{r+1}' + c_{3,r} f_{r+1}' + c_{4,r} f_{r+1} + c_{5,r} g_{r+1}' + c_{6,r} g_{r+1} \\ = c_{7,r} \end{aligned} \quad (14)$$

where the coefficients  $a_{s,r}$ ,  $s = 1, 2, \dots$  are known functions calculated from previous iterations and are defined as

$$a_{1,r} = \frac{4\lambda}{1-N}, \quad a_{2,r} = \frac{2N\lambda}{1-N}, \quad a_{3,r} = \sqrt{\lambda} g_s,$$

$$b_{1,r} = \frac{2(2-N)\lambda}{m^2}, \quad b_{2,r} = \frac{4-2N}{m^2},$$

$$c_{1,r} = \lambda^3, \quad c_{2,r} = \lambda^2, \quad c_{3,r} = \frac{Br}{1-N} [\lambda^2 N f_r' - \lambda^2 N g_r + 2\lambda^2 f_r' - 2\lambda f_r'],$$

$$c_{4,r} = \frac{2Br}{1-N} (f_r - \lambda f_r'), \quad c_{5,r} = \left(\frac{2BrN}{1-N}\right) \left(\frac{2-N}{m^2}\right) \lambda^3 g_r',$$

$$c_{6,r} = \frac{BrN}{1-N} \lambda^2 (g_r - f_r'),$$

$$c_{7,r} = \frac{Br}{1-N} \left[ \frac{N}{2} \lambda^2 (f_r' - g_r)^2 + (f_r - \lambda f_r')^2 + N \left( \frac{2-N}{m^2} \right) \lambda^3 g_r'^2 \right]. \quad (15)$$

The above linearized Eqs. (12)–(14) are solved using the Chebyshev spectral collocation method [31]. The unknown functions are approximated by the Chebyshev interpolating polynomials in such a way that they are collocated at the Gauss–Lobatto points defined as

$$\xi_j = \cos \frac{\pi j}{J}, \quad j = 0, 1, 2, \dots, J \quad (16)$$

where  $J$  is the number of collocation points used. The physical region  $[\lambda_0, 1]$  is transformed into the region  $[-1, 1]$  using the mapping

$$\lambda = \frac{(1 - \lambda_0)\xi + (1 + \lambda_0)}{2}, \quad -1 \leq \xi \leq 1 \quad (17)$$

The functions  $f_{r+1}$ ,  $g_{r+1}$  and  $\theta_{r+1}$  are approximated at the collocation points by

$$\begin{aligned} f_{r+1}(\xi) &= \sum_{k=0}^J f_{r+1}(\xi_k) T_k(\xi), \quad g_{r+1}(\xi) = \sum_{k=0}^J g_{r+1}(\xi_k) T_k(\xi), \\ \theta_{r+1}(\xi) &= \sum_{k=0}^J \theta_{r+1}(\xi_k) T_k(\xi) \end{aligned} \quad (18)$$

$$j = 0, 1, 2, \dots, J$$

where  $T_k$  is the  $k^{\text{th}}$  Chebyshev polynomial defined by

$$T_k(\xi) = \cos[k \cos^{-1} \xi] \quad (19)$$

The basic idea behind the Chebyshev-spectral collocation method is the introduction of a differentiation matrix  $D$  which is used to approximate the derivatives of the unknown variables  $f_{r+1}$ ,  $g_{r+1}$ ,  $\theta_{r+1}$  at the collocation points as the matrix vector product.

The derivatives of the variables at the collocation points are represented as

$$\begin{aligned} \frac{d^n f_{r+1}}{d\lambda^n} &= \sum_{k=0}^J \mathbf{D}_{jk}^n f_{r+1}(\xi_k), \quad \frac{d^n g_{r+1}}{d\lambda^n} = \sum_{k=0}^J \mathbf{D}_{jk}^n g_{r+1}(\xi_k), \\ \frac{d^n \theta_{r+1}}{d\lambda^n} &= \sum_{k=0}^J \mathbf{D}_{jk}^n \theta_{r+1}(\xi_k) \end{aligned} \quad (20)$$

$$j = 0, 1, 2, \dots, J$$

where  $n$  is the order of differentiation and  $\mathbf{D} = \frac{2D}{(1-\lambda_0)}$  being the Chebyshev spectral differentiation matrix. Substituting Eqs. (17)–(20) into Eqs. (12)–(14) leads to the matrix equation:

$$\mathbf{A}_r \mathbf{X}_{r+1} = \mathbf{B}_r \quad (21)$$

In Eq. (21),  $\mathbf{A}_r$  is a  $(3J + 3) \times (3J + 3)$  square matrix and  $\mathbf{X}_{r+1}$  and  $\mathbf{B}_r$  are  $(3J + 3) \times 1$  column vectors defined by

$$\mathbf{A}_r = \begin{bmatrix} A_{11} & A_{12} & A_{13} \\ A_{21} & A_{22} & A_{23} \\ A_{31} & A_{32} & A_{33} \end{bmatrix}, \quad \mathbf{X}_{r+1} = \begin{bmatrix} \mathbf{F}_{r+1} \\ \mathbf{G}_{r+1} \\ \mathbf{\Theta}_{r+1} \end{bmatrix}, \quad \mathbf{B}_r = \begin{bmatrix} \mathbf{r}_{1,r} \\ \mathbf{r}_{2,r} \\ \mathbf{r}_{3,r} \end{bmatrix} \quad (22)$$

where

$$\mathbf{F}_{r+1} = [f_{r+1}(\xi_0), f_{r+1}(\xi_1), \dots, f_{r+1}(\xi_{J-1}), f_{r+1}(\xi_J)]^T,$$

$$\begin{aligned}
\mathbf{G}_{r+1} &= [g_{r+1}(\xi_0), g_{r+1}(\xi_1), \dots, g_{r+1}(\xi_{J-1}), g_{r+1}(\xi_J)]^T, \\
\Theta_{r+1} &= [\theta_{r+1}(\xi_0), \theta_{r+1}(\xi_1), \dots, \theta_{r+1}(\xi_{J-1}), \theta_{r+1}(\xi_J)]^T, \\
A_{11} &= a_{1,r} \mathbf{D}^2, \quad A_{12} = -a_{2,r} \mathbf{D}, \quad A_{13} = a_{3,r} \mathbf{I}, \quad A_{21} = \mathbf{D}, \\
A_{22} &= b_{1,r} \mathbf{D}^2 + b_{2,r} \mathbf{D} - \mathbf{I}, \quad A_{23} = \mathbf{0}, \\
A_{31} &= c_{3,r} \mathbf{D} + c_{4,r} \mathbf{I}, \quad A_{32} = c_{5,r} \mathbf{D} + c_{6,r} \mathbf{I}, \quad A_{33} = c_{1,r} \mathbf{D}^2 + c_{2,r} \mathbf{D}, \\
\mathbf{r}_{1,r} &= \mathbf{0}_1, \quad \mathbf{r}_{2,r} = \mathbf{0}_1, \quad \mathbf{r}_{3,r} = c_{7,r}.
\end{aligned} \quad (23)$$

Here  $\mathbf{I}$  and  $\mathbf{0}$  represents  $(J+1) \times (J+1)$  identity matrix and zero matrix respectively.

The corresponding boundary conditions are as follows:

$$\begin{aligned}
-2\alpha\lambda_0 \sum_{k=0}^J \mathbf{D}_{jk} f_{r+1}(\xi_k) + (\sqrt{\lambda_0} + 2\alpha) f_{r+1}(\xi_J) &= 0; \\
g_{r+1}(\xi_J) = 0; \quad Bi\theta_{r+1}(\xi_J) &= 2\sqrt{\lambda_0} \sum_{k=0}^J \mathbf{D}_{jk} \theta_{r+1}(\xi_k); \quad (24a) \\
2\alpha \sum_{k=0}^J \mathbf{D}_{0k} f_{r+1}(\xi_k) + (1-2\alpha) f_{r+1}(\xi_0) &= b; \quad g_{r+1}(\xi_0) = \left[ \frac{df}{d\lambda} \right]_{\lambda=1}; \\
Bi\theta_{r+1}(\xi_0) &= Bi - 2 \sum_{k=0}^J \mathbf{D}_{0k} \theta_{r+1}(\xi_k); \quad (24b)
\end{aligned}$$

After modifying the matrix system (21) to incorporate boundary conditions (24), the solution is obtained as

$$\mathbf{X}_{r+1} = \mathbf{A}_r^{-1} \mathbf{B}_r \quad (25)$$

The initial approximations  $f_0$ ,  $g_0$  and  $\theta_0$  are chosen to be functions that satisfy the boundary conditions (24) i.e.

$$\begin{aligned}
f_0(\lambda) &= \frac{(-b\lambda_0\sqrt{\lambda_0}) + b(\sqrt{\lambda_0} + 2\alpha)\lambda}{\sqrt{\lambda_0}(1-\lambda_0) + 2\alpha(1+\lambda_0\sqrt{\lambda_0})}, \\
g_0(\lambda) &= \frac{b(\sqrt{\lambda_0} + 2\alpha)(\lambda_0 - \lambda)}{(\sqrt{\lambda_0}(1-\lambda_0) + 2\alpha(1+\lambda_0\sqrt{\lambda_0}))(\lambda_0 - 1)}, \\
\theta_0(\lambda) &= \frac{2\sqrt{\lambda_0} - Bi\lambda_0 + Bi\lambda}{2(\sqrt{\lambda_0} + 1) + Bi(1-\lambda_0)} \quad (26)
\end{aligned}$$

#### 4. Entropy generation

The volumetric rate of entropy generation for incompressible micropolar fluid [24] is given as

$$\begin{aligned}
S_G &= \frac{K_f}{T_a^2} \left( \frac{\partial T}{\partial r} \right)^2 + \frac{\mu + \kappa}{T_a} \left[ r \frac{\partial}{\partial r} \left( \frac{u}{r} \right) \right]^2 \\
&\quad + \frac{2\kappa}{T_a} \left[ \frac{1}{2r} \frac{\partial}{\partial r} (ru) - \Gamma \right]^2 + \frac{\gamma}{T_a} \left( \frac{\partial \Gamma}{\partial r} \right)^2 \quad (27)
\end{aligned}$$

According to Bejan [6], the dimensionless entropy generation number  $N_s$  is the ratio of the volumetric entropy generation rate to the characteristic entropy generation rate. Thus the entropy generation number is given by

$$\begin{aligned}
N_s &= 4\lambda \left( \frac{d\theta}{d\lambda} \right)^2 + \frac{4Br}{T_p} \left[ \frac{1}{1-N} \left( \frac{df}{d\lambda} - \frac{f}{\lambda} \right)^2 + \frac{N}{2(1-N)} \left( \frac{df}{d\lambda} - g \right)^2 \right. \\
&\quad \left. + \frac{N\lambda}{1-N} \left( \frac{2-N}{m^2} \right) \left( \frac{dg}{d\lambda} \right)^2 \right] \quad (28)
\end{aligned}$$

where  $T_p = \frac{T_b - T_a}{T_a}$  is the dimensionless temperature difference and the characteristic entropy generation rate is  $\frac{K_f(T_b - T_a)^2}{T_a^2}$ . The Eq. (28) can be expressed alternatively as follows:

$$N_s = N_h + N_v \quad (29)$$

The first term on the right hand side of this equation denotes the entropy generation due to heat transfer irreversibility and the second term represents the entropy generation due to viscous dissipation.

To evaluate the irreversibility distribution, the parameter  $Be$  (Bejan number), which is the ratio of entropy generation due to heat transfer to the overall entropy generation (29) is defined as follows:

$$Be = \frac{N_h}{N_h + N_v} \quad (30)$$

The Bejan number varies from 0 to 1. Subsequently,  $Be = 0$  reveals that the irreversibility due to viscous dissipation dominates, whereas  $Be = 1$  indicates that the irreversibility due to heat transfer is dominant. It is obvious that the  $Be = 0.5$  is the case in which the irreversibility due to heat transfer is equal to viscous dissipation in the entropy production.

#### 5. Results and discussion

The case of Newtonian fluid flow between concentric cylinders of Sinha and Chaudhary [32] can be obtained by taking  $N = 0$ ,  $gs = 0$ ,  $m = 0$ ,  $Br = 0$  and  $\alpha = 0$ . Thus, in order to assess the accuracy of our method, the results of the present problem, in the absence of  $N$ ,  $gs$ ,  $m$ ,  $Br$ ,  $\alpha$ , have been compared with the analytical solution of Sinha and Chaudhary [32] for Newtonian fluids. The comparison in the above case is found to be in good agreement, as shown in Table 1.

The micropolar fluid flow through a concentric cylindrical annulus with slip and convective boundary conditions are analyzed in this paper. Entropy generation in the flow field due to fluid friction and heat transfer is formulated. The influence of various parameters on velocity, microrotation, temperature, entropy generation and Bejan number is examined. To study the effects of  $N$ ,  $Br$ ,  $\alpha$  and  $Bi$ , computations were carried out by taking  $m = 2$ ,  $gs = 1$ ,  $a = 0.5$ ,  $b = 1$ .

**Table 1** Comparison analysis for the velocity calculated by the present method and that of analytical solution [32] for  $\alpha = 0$ .

$\lambda$	Analytical solution [32]	Present solution
1	1	1
0.9816	0.97546	0.975468
0.9284	0.90453	0.904529
0.8454	0.79386	0.793863
0.7409	0.65453	0.654539
0.625	0.5	0.5
0.5091	0.34546	0.345462
0.4046	0.20613	0.206127
0.3216	0.09546	0.095462
0.2684	0.02453	0.024532
0.25	0	0



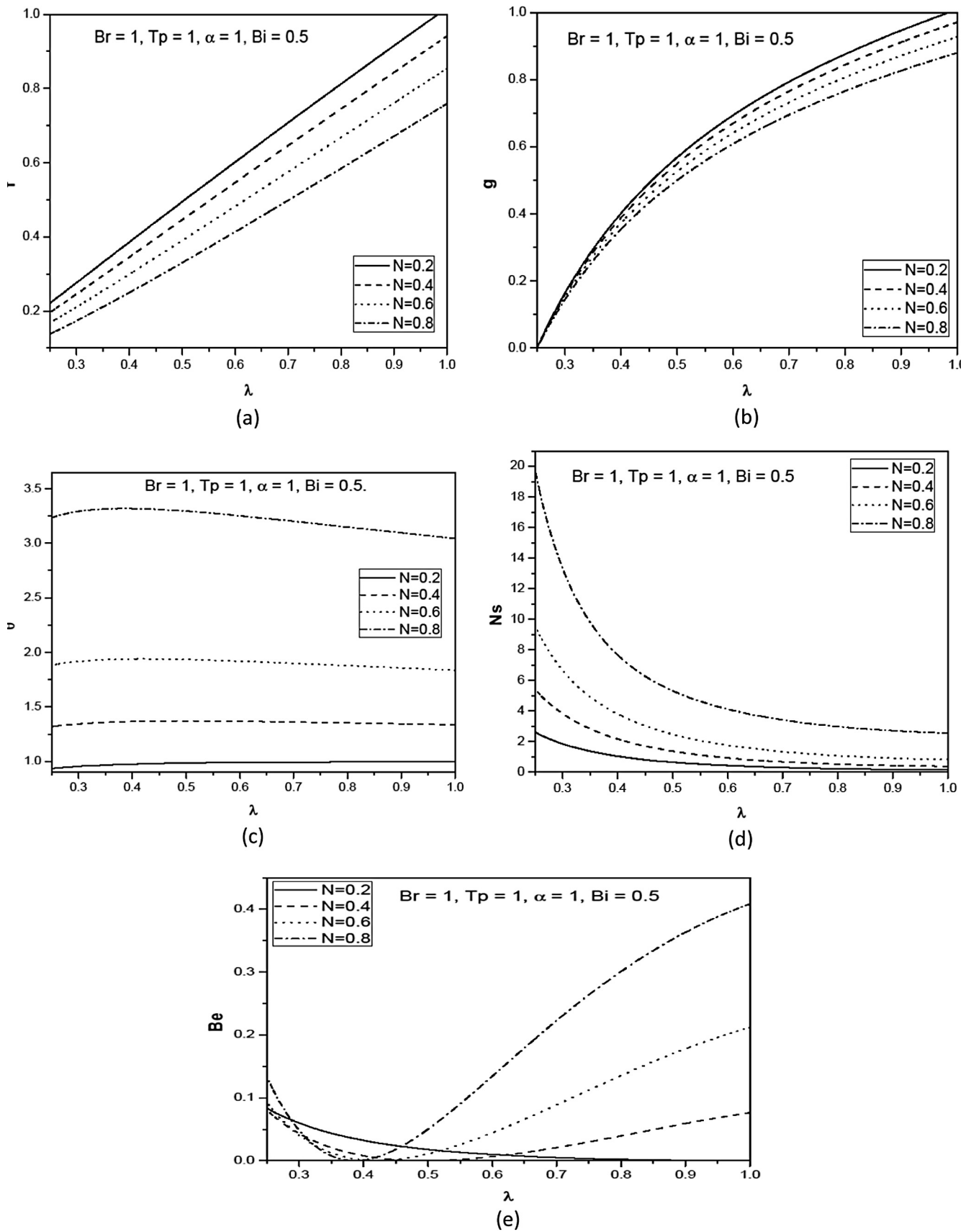


**Figure 2** Effect of coupling number on (a) velocity ( $f$ ), (b) micro rotation ( $g$ ), (c) temperature ( $\theta$ ), (d) entropy generation ( $N_s$ ) and (e) Bejan number ( $Be$ ).

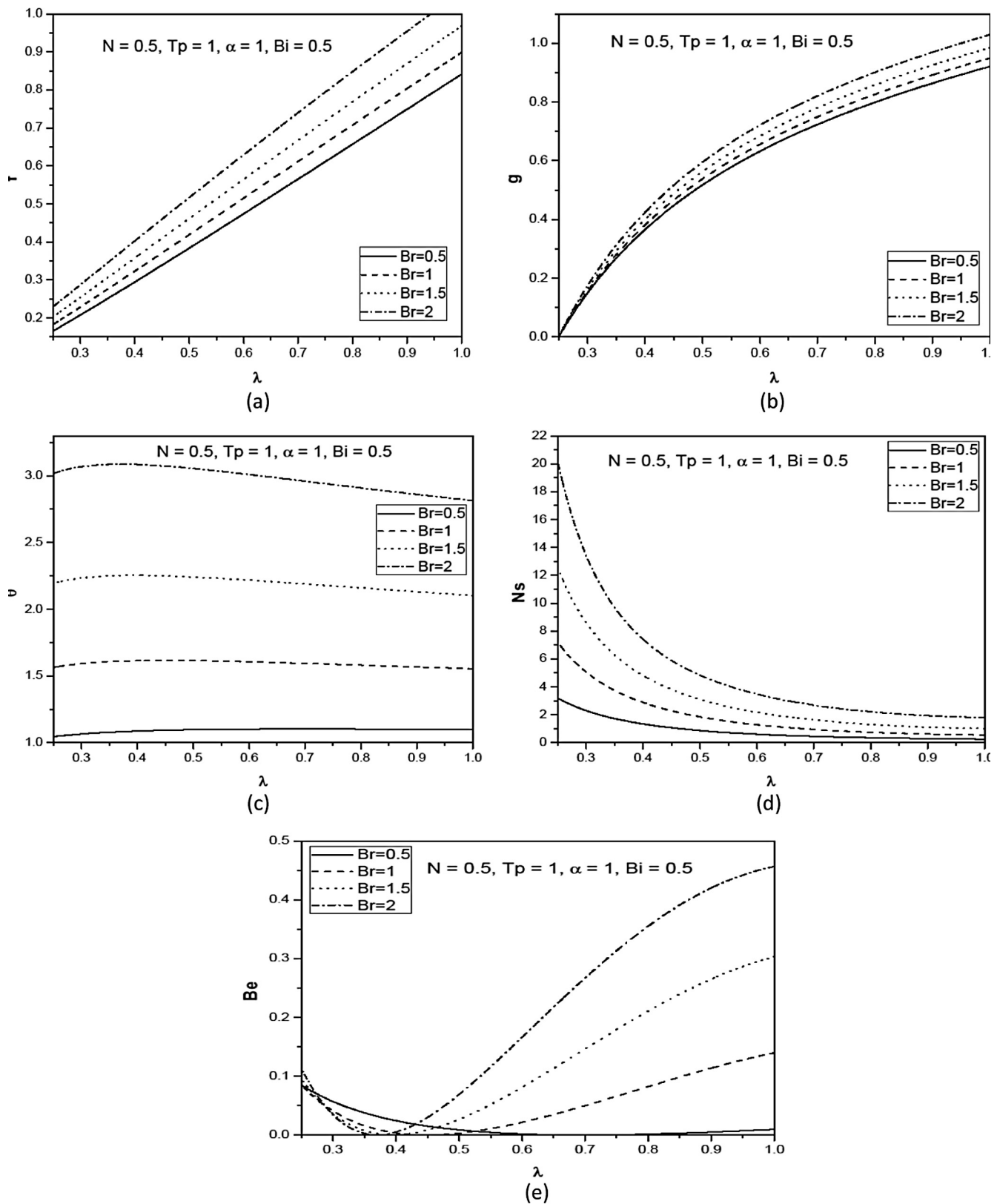


**Figure 3** Effect of Brinkman number on (a) velocity ( $f$ ), (b) micro rotation ( $g$ ), (c) temperature ( $\theta$ ), (d) entropy generation ( $N_s$ ) and (e) Bejan number ( $Be$ ).

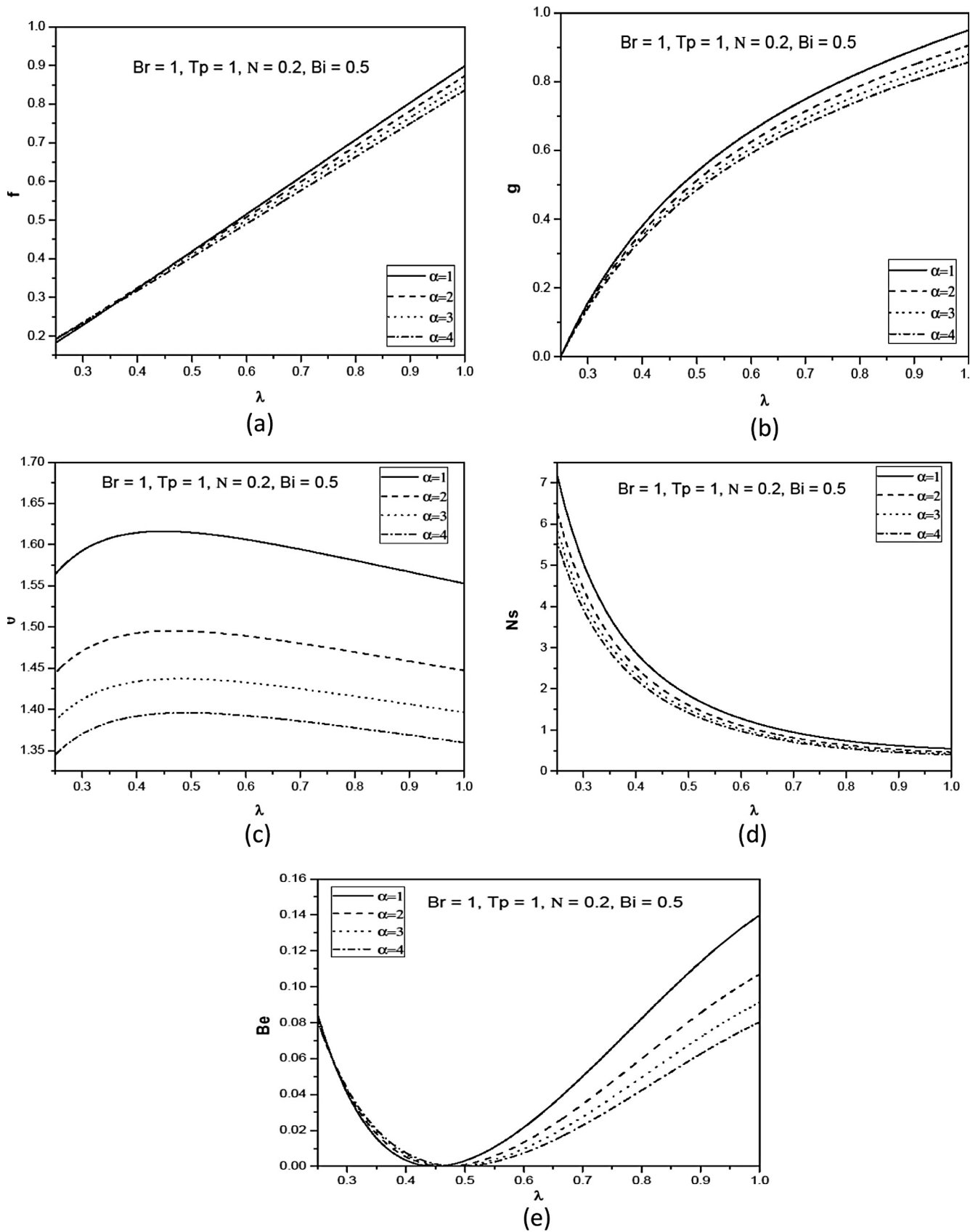


**Figure 4** Effect of slip parameter on (a) velocity ( $f$ ), (b) micro rotation ( $g$ ), (c) temperature ( $\theta$ ), (d) entropy generation ( $N_s$ ) and (e) Bejan number ( $Be$ ).



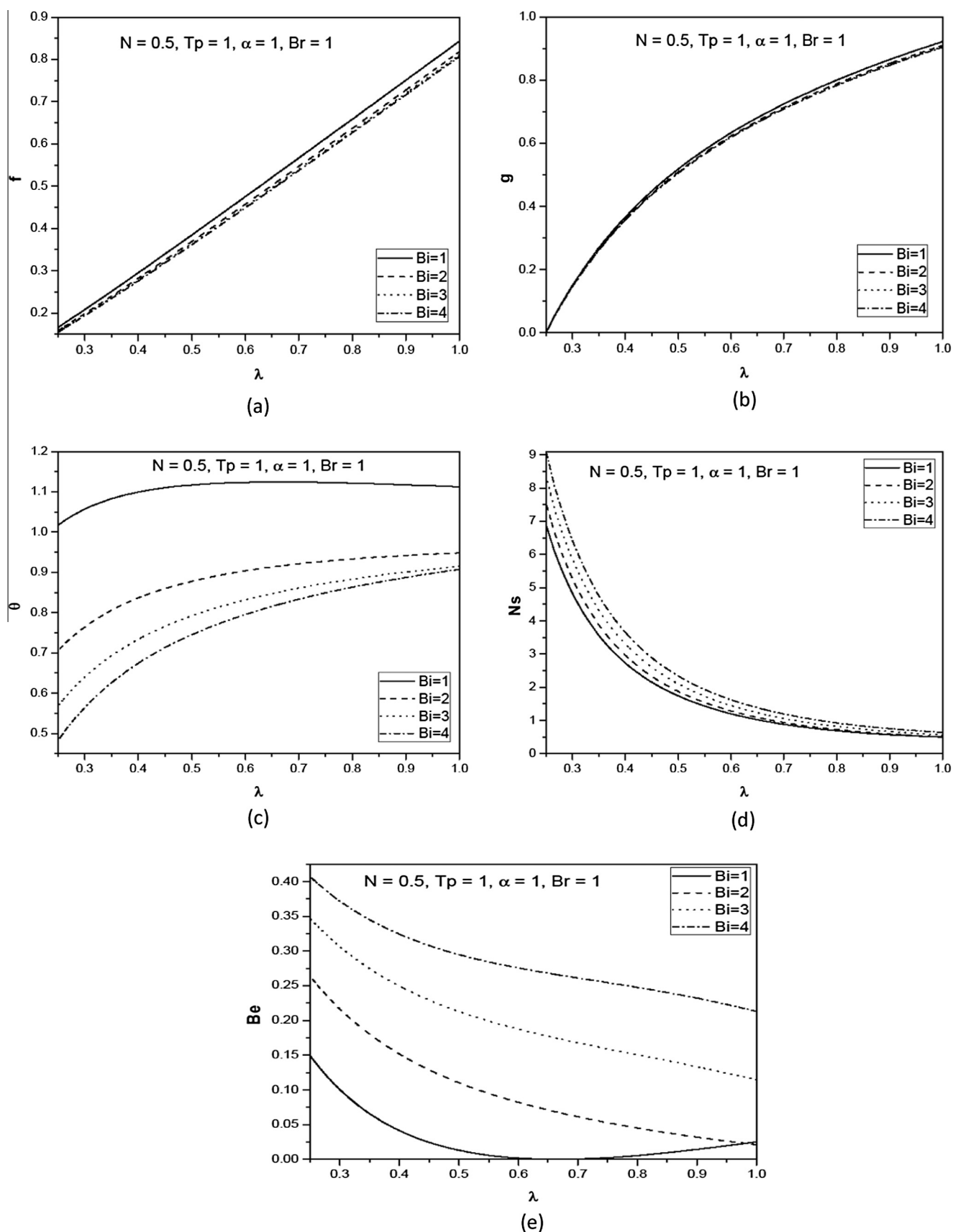


**Figure 5** Effect of Biot number on (a) velocity ( $f$ ), (b) micro rotation ( $g$ ), (c) temperature ( $\theta$ ), (d) entropy generation ( $N_s$ ) and (e) Bejan number ( $Be$ ).

Fig. 2 presents the effect of coupling number ( $N$ ) on non-dimensional velocity, micro rotation, temperature, entropy generation and Bejan number. The coupling of linear and rotational motion arising from the micromotion of the fluid molecules is characterized by coupling number. Hence,  $N$  signifies the coupling between the Newtonian and rotational viscosities. As  $N \rightarrow 1$ , the effect of microstructure becomes significant, whereas with a small value of  $N$  the individuality of the sub-structure is much less pronounced. As  $\kappa \rightarrow 0$  i.e.  $N \rightarrow 0$ , the micropolarity is lost and the fluid behaves as nonpolar fluid. Hence,  $N \rightarrow 0$  corresponds to viscous fluid. Fig. 2(a) shows that the velocity decreases as  $N$  increases. Fig. 2(b) depicts that, the microrotation component decreases with increase in the value of  $N$ . Fig. 2(c) reveals that as  $N$  increases temperature increases. In Fig. 2(d) it is observed that the entropy generation increases as coupling number increases. Fig. 2(e) reveals that the Bejan number  $Be$  decreases near the inner cylinder and increases near the outer cylinder with increase in the coupling number  $N$ .

The effect of Brinkman number on the velocity, microrotation, temperature, entropy generation and Bejan number is shown in Fig. 3. Fig. 3(a) shows that the velocity increases with increase in the value of  $Br$ . Fig. 3(b) shows that the microrotation increases as  $Br$  increases. It is noticed from Fig. 3(c) and (d) that the temperature and entropy generation increase as  $Br$  increases. For all parameters, the inner cylinder acts as a strong concentrator of irreversibility. Entropy generation number is high in magnitude near the inner cylinder due to the presence of high temperature and velocity gradients.  $N_s$  then falls exponentially along the radial direction, approaching an asymptote near the outer cylinder. Entropy generation profiles are similar in shape and almost parallel to one another for all the parameter variations, but they vary in magnitudes. It is noticed from Fig. 3(e) that as  $Br$  increases, the Bejan number decreases at the inner cylinder which indicates that the fluid friction contribution to entropy generation increases. It is also observed that the Bejan number increases near the outer cylinder due to high heat transfer contribution.

Fig. 4(a)–(d) illustrates the effect of slip parameter on the velocity, microrotation, temperature and entropy generation. It is observed that the slip parameter  $\alpha$  has significant influence on all the parameters. As  $\alpha$  increases velocity, microrotation, temperature and entropy generation decrease. It is noticed from Fig. 4(e) that there is no significant effect on Bejan number near the inner but near the outer cylinder the Bejan number decreases as  $\alpha$  increases.

Fig. 5 shows the velocity, micro rotation, temperature, entropy generation and Bejan number profiles for different values of the Biot number. Physically, Biot number is expressed as the convection at the surface of the body to the conduction within the surface of the body. Here we have assumed the convective heat transfer coefficients ( $h_1$ ,  $h_2$ ) are same at the inner and outer cylinders i.e.  $Bi_1 = Bi_2 = Bi$ . It is observed from Fig. 5(a) that increase in Biot number decrease the velocity profile of the fluid in an annular space. It is due to the fact that Biot number reduces the heat transfer rate in the cylinder walls. Fig. 5(b) shows that the microrotation decreases as  $Bi$  increases. Decrease in temperature is noticed with a rise in Biot number due to a convective cooling at the cylinders as shown in Fig. 5(c). Fig. 5(d) reveals that the entropy generation increases as  $Bi$  increases. The effect of Biot

number  $Bi$  on  $Be$  is shown in Fig. 5(e). As Biot number increases  $Be$  also increases.

## 6. Conclusions

The effect of slip and convective boundary conditions on the entropy generation of fully developed micropolar fluid flow between concentric cylinders is investigated numerically by Spectral Quasi linearization method. From the present investigation the following conclusions are drawn:

- Near the inner cylinder, the entropy generation rate is higher due to the presence of high temperature and velocity gradients. Entropy generation rate shows an asymptotic behavior toward the outer cylinder.
- At the inner cylinder, Bejan number decreases along the radial direction to a minimum value, and then increases slightly toward the outer cylinder.
- As  $Br$  increases, the entropy generation increases due to the Contribution of the fluid friction.
- The maximum value of Bejan number (i.e. maximum heat transfer irreversibility) is observed at the outer cylinder.
- The effect of slip parameter  $\alpha$  is to reduce the entropy generation rate and Bejan number.
- As the Biot number  $Bi$  increases, entropy generation increases in the entire region.

## Acknowledgment

The authors gratefully acknowledge the referees for their constructive comments and valuable suggestions.

## References

- [1] Taylor GI. Distribution of velocity and temperature between concentric rotating cylinders. Proc Roy Soc London – Ser-A 1935;151:494–512.
- [2] Hessami MA, Vaw Davis GD, Reizes JAE. Int J Heat Mass Transf 1987;30.
- [3] Borjini MN, Mbow Cheikh, Dagenet Michel. Numerical analysis of combined radiation and unsteady natural convection within a horizontal annular space. Int J Num Meth Heat Fluid Flow 1999;9(7):742–63.
- [4] Atayilmaz SO. Experimental and numerical study of natural convection heat transfer from horizontal concentric cylinders. Int J Thermal Sci 2011;50:1472–83.
- [5] Deka RK, Paul A. Stability of dean flow between two porous concentric cylinders with radial flow and a constant heat flux at the inner cylinder. J Fluids Eng 2013;135, 041203-1-8.
- [6] Bejan A. A study of entropy generation in fundamental convective heat transfer. J Heat Transfer 1979;101:718–25.
- [7] Sahin AZ. Second law analysis of laminar viscous flow through a duct subjected to constant wall temperature. J Heat Transfer 1998;120:76–83.
- [8] Tasnim SH, Mahmud S. Entropy generation in a vertical concentric channel with temperature dependent viscosity. Int Comm Heat Mass Transfer 2002;29(7):907–18.
- [9] Haddad OM, Alkam MK, Khasawneh MT. Entropy generation due to laminar forced convection in the entrance region of a concentric annulus. Energy 2004;29:35–55.
- [10] Yari M. Second-law analysis of flow and heat transfer inside a microannulus. Int Comm Heat Mass Transfer 2009;36:78–87.

- [11] Chen S, Liu Z, Zheng C. Natural convection and entropy generation in a vertically concentric annular space. *Int J Thermal Sci* 2010;49:2439–52.
- [12] Assad MEH, Oztop HF. Parametric study of entropy generation in a fluid with internal heat generation between two rotating cylinders subjected to convective cooling at the surface. *ISRN Chem Eng* 2012;2012:1–9.
- [13] Mazgar A, Ben Nejma F, Charrada K. Second law analysis of coupled mixed convection and non-grey gas radiation within a cylindrical annulus. *Int J Math Models Methods Appl Sci* 2013;7:265–76.
- [14] Eegunjobi AS, Makinde OD. Entropy generation analysis in transient variable viscosity Couette flow between two concentric pipes. *J Thermal Sci Technol* 2014;9(2):1–10.
- [15] Rashidi MM, Kavyani N, Abelman S. Investigation of entropy generation in MHD and slip flow over a rotating porous disk with variable properties. *Int J Heat Mass Transf* 2014;70:892–917.
- [16] Das S, Jana RN, Chamkha AJ. Entropy generation in a rotating Couette flow with suction/injection. *Commun Numer Anal* 2015;2015(1):62–81.
- [17] Yilbas BS, Yurusoy M, Pakdemirli M. Entropy analysis for non-Newtonian fluid flow in annular pipe: constant viscosity case. *Entropy* 2004;6:304–15.
- [18] Kahraman A, Yurusoy M. Entropy generation due to non-newtonian fluid flow in annular pipe with relative rotation: constant viscosity case. *J Theor Appl Mech* 2008;46(1):69–83.
- [19] Mirzazadeh M, Shafaei A, Rashidi F. Entropy analysis for non-linear viscoelastic fluid in concentric rotating cylinders. *Int J Thermal Sci* 2008;47:1701–11.
- [20] Mahian O, Mahmud S, Heris SZ. Analysis of entropy generation between co-rotating cylinders using nanofluids. *Energy* 2012;44:438–46.
- [21] Kim S, Zhang Y, Choi J. Entropy generation analysis for a pulsating heat pipe. *Heat Transfer Res* 2013;44(1):1–30.
- [22] Chen C, Chen B, Liu C. Heat transfer and entropy generation in fully-developed mixed convection nanofluid flow in vertical channel. *Int J Heat Mass Transf* 2014;79:750–8.
- [23] Mkwizu MH, Makinde OD. Entropy generation in a variable viscosity channel flow of nanofluids with convective cooling. *C R Mec* 2015;343(1):38–56.
- [24] Das S, Banu AS, Jana RN, Makinde OD. Entropy analysis on MHD pseudo-plastic nanofluid flow through a vertical porous channel with convective heating. *Alexandria Eng J* 2015;54(3):325–37.
- [25] Eringen AC. *Microcontinuum field theories II, fluent media*. New York: Springer; 2001.
- [26] Chen CK, Yang Y, Hachang K. The effect of thermal radiation on entropy generation due to micro-polar fluid flow along a wavy surface. *Entropy* 2011;13:1595–610.
- [27] Ramana Murthy JV, Srinivas J. Second law analysis for Poiseuille flow of immiscible micropolar fluids in a channel. *Int J Heat Mass Transf* 2013;65:254–64.
- [28] Kazakia Y, Ariman T. Heat conducting micropolar fluids. *Rheol Acta* 1971;10:319–25.
- [29] Ramkissoon H, Majumdar SR. Unsteady flow of a micropolar fluid between two concentric circular cylinders. *Can J Chem Eng* 1977;55:408–13.
- [30] Bellman RE, Kalaba RE. *Quasilinearisation and non-linear boundary-value problems*. New York, NY, USA: Elsevier; 1965.
- [31] Canuto C, Hussaini MY, Quarteroni A, Zang TA. *Spectral methods fundamentals in single domains*. Springer Verlag; 2006.
- [32] Sinha KD, Chaudhary RC. Viscous incompressible flow between two coaxial rotating porous cylinders. *Proc Nat Inst Sci* 1966;32:81–8.



**Dr. D. Srinivasacharya** completed his Ph.D. (Mathematics) at Regional Engineering College (N.I.T.) Warangal, Telangana India, in the year 1996. His research interests are Fluid Mechanics, Computational Fluid Dynamics and Bio-Fluid Mechanics. He published about 100 papers in various reputed journals and supervised 11 Ph.D. students and guiding 5 more; completed 4 research projects; and reviewed research articles in various national and international journals.



**Mrs. K. Hima Bindu** pursuing her Ph.D. (Mathematics) at National Institute of Technology, Warangal, Telangana, India. Her research interests are Fluid Mechanics and Computational Fluid Dynamics.